Cure Kinetic Study of Epoxidized Hemp Oil Cured with a Multiple Catalytic System

Nathan W. Manthey, Francisco Cardona, Thiru Aravinthan

Centre of Excellence in Engineered Fibre Composites (CEEFC), Faculty of Engineering and Surveying, University of Southern Queensland, Toowoomba, Queensland 4350, Australia

Received 14 June 2011; accepted 1 September 2011
DOI 10.1002/app.35561
Published online in Wiley Online Library (wileyonlinelibrary.com).

ABSTRACT: The cure kinetics of two epoxidized hemp oil (EHO) based bioresins were studied and compared under both dynamic and isothermal conditions using differential scanning calorimetry (DSC). Neat triethylenetetramine (TETA) for the first system and a combination of isophorone diamine (IPD) and TETA for the second system were used as the hardeners for the two EHO-based bioresins. Lower total heats of reaction and an approximate 10% decrease in activation energies were observed for the IPD/TETA system. Maximum conversions of the TETA/IPD system were consistently higher than those of the TETA system throughout the entire temperature range suggesting enhanced curing characteristics. Kissinger and Ozawa–Flynn–Wall models were used to determine activation energies from dynamic DSC data. Both bioresin systems were found to display autocatalytic behavior with the TETA/IPD system showing high *n*th order influence. Kamal's autocatalytic isothermal model, modified to account for diffusion postvitrification was found to satisfactorily describe the cure behavior of both bioresin systems. Overall, the addition of IPD was found to increase the curing rate of the EHO bioresin systems. © 2012 Wiley Periodicals, Inc. J Appl Polym Sci 000: 000–000, 2012

Key words: biopolymers; curing of polymers; differential scanning calorimetry (DSC); kinetics (polym.); renewable resources

INTRODUCTION

Increasing environmental awareness pertaining to the use of petrochemically derived polymer resins in the fiber composite industry is propelling the development of bioresins based on renewable, natural materials. These bioresins are an emerging sustainable thermoset technology often derived from vegetable oils and are termed epoxidized vegetable oils (EVO). Because of their biological origin they represent a sustainable, low-environmental impact option to existing petrochemically derived resins.

The majority of EVO bioresin research has focused on the mechanical characterization and moisture absorption of bioresins and biocomposites utilizing said bioresins.[1–6] Although a large body of literature has been published on cure kinetic studies of synthetic resins,[7–18] the curing kinetics of EVO bioresins is under represented. Several studies have been conducted by Liang and Chandrashekhara[19] and Liang et al.[20] focusing on the cure kinetics and rheology analysis of soybean oil based bioresins. Park et al.[21] performed cure characterization of ESO and epoxidized castor oil (ECO) that involved examining the degree of cure as a function of temperature. In our previous publication, the cure behavior of an EHO-based bioresin system was studied using dynamic and isothermal cure kinetics.[22] Owing to the numerous types of vegetable oils and the great potential they hold as bioresin feedstocks it is essential to study the curing behavior, specifically the cure kinetics of novel vegetable oil based bioresins such as epoxidized hemp oil (EHO).

Hemp oil is currently treated as a by-product of hemp fiber production. Given this fact and its unique fatty acid profile, high in both linoleic and linolenic acid; hemp oil holds significant potential as a bioresin feedstock. Because of the potential and novelty of hemp oil based bioresins further investigation and characterization is justified.

In this article, differential scanning calorimetry (DSC) was utilized in the study of the cure kinetics through both dynamic and isothermal analysis. Both Kissinger and Ozawa–Flynn–Wall dynamic models and Kamal's autocatalytic isothermal model were used to study and compare the curing of EHO-based bioresins with first, triethylenetetramine (TETA) and second, a combination of isophorone diamine (IPD) and TETA as the curing agents.

Correspondence to: N. W. Manthey (nathan.manthey@usq.edu.au).

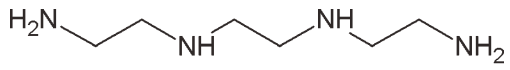

Triethylenetetramine (TETA)

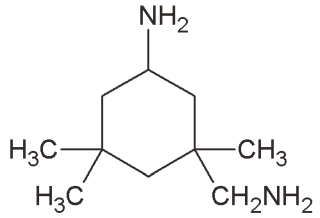

Isophorone Diamine (IPD)

Figure 1 Molecular structures of triethylenetetramine (TETA) and isophorone diamine (IPD).

EXPERIMENTAL

Materials

The studied bioresins are based on EHO which was synthesized at the Centre of Excellence in Engineered Fibre Composites (CEEFC). Cold pressed raw industrial hemp oil was supplied by Ecofibre (Maleny, Queensland, Australia) with a fatty acid profile consisting of the following acids: palmitic = 6.0%; stearic = 2.0%; oleic = 12.0%; linoleic = 57.0%; linolenic = 20.7%; and other = 2.3%. Listed iodine number = 165 (g I/100 g oil); saponification value = 193.

IPD (Amine hydrogen equivalent weight (AHEW) $\approx$ 42.6), supplied from ATL composites (Southport, Queensland, Australia) and TETA (AHEW $\approx$ 24), from Huntsman was used as supplied, Figure 1. Analytical grade glacial acetic acid and hydrogen peroxide with minimum concentrations of 99.7% and 30%, respectively, were used as received from Lab-Serv (Biolab, Australia). Amberlite IR-120 was used as received from Fluka (Sigma–Aldrich, Australia) and was of the ionic H^+ form.

A Mettler Toledo LabMax automatic reactor with a 4 L four-necked reaction vessel equipped with a mechanical "ship anchor" stirrer and thermometer was used for the epoxidation procedure.

Methods

In situ epoxidation of hemp oil

EHO was synthesized through the epoxidation of cold pressed raw industrial hemp oil (156.25 g, 1 mol) by peroxyacetic acid, formed *in situ* by the reaction of hydrogen peroxide (113.4 g, 1 mol) and acetic acid (40.04 g, 0.67 mol) in the presence of an acidic ion exchange resin, Amberlite IR-120 H^+ (15% by weight of hemp oil) as the catalyst, Figure 2. The constituents were added to a four-necked reaction vessel equipped with a mechanical stirrer and thermometer. Stirring was initiated and the reactor temperature was increased until the mixture reached 40°C whereby dropwise addition of hydrogen peroxide was performed over a period of 1 h. Temperature and stirring speed were then increased to operational values of 75°C and 110 rpm, respectively. These parameters were maintained for a period of 7 h.

On completion of the reaction, the catalyst was filtered off and the reactor contents were cleaned in a separation funnel by washing with water three times (cool, near-boiling, and cool) to remove the aqueous phase. Next, the resin was centrifuged and aerated to remove any remaining water. The resin was then further dried through the addition of anhydrous sodium sulfate in the proportion of 0.15 g per 1 g of resin. Following the addition of anhydrous sodium sulfate, the resin was placed in an oven at 70°C for 12 h and subsequently filtered through Whatman No. 4 filter paper. Oxirane oxygen content was determined by titration to be 8.2%. The yield of EHO obtained was $\sim$ 75%. At room temperature, EHO is a yellow colored liquid with a slight vegetable oil odor.

Curing kinetics of EHO-TETA and EHO-TETA-IPD using DSC

A calibrated TA Instruments DSC Q100 with Universal Analysis 2000 version 3.9A software was used for the dynamic and isothermal analysis. Dry nitrogen

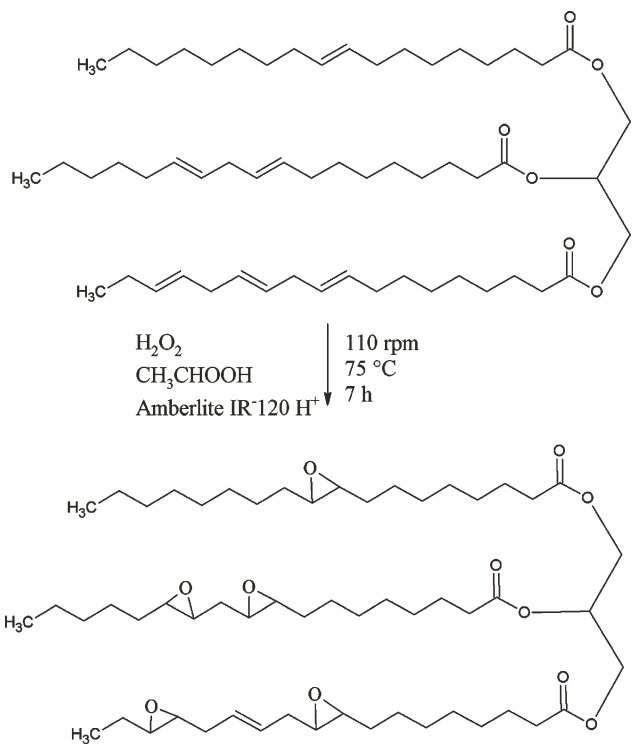

Figure 2 *In situ* epoxidation of hemp oil.

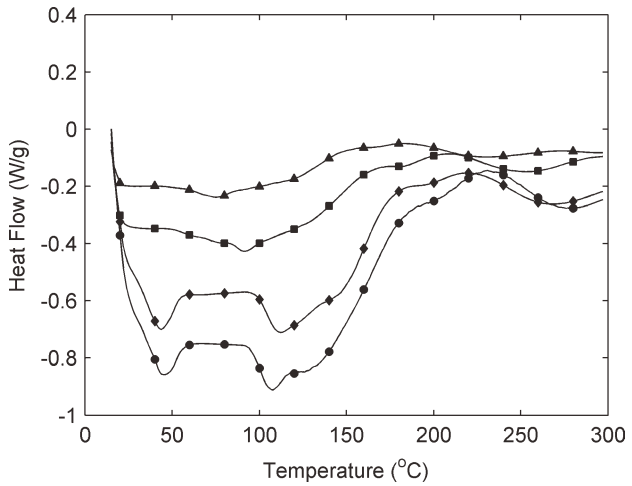

Figure 3 Dynamic DSC thermograms for EHO/TETA with 5°C/min (▲), 10°C/min (■), 15°C/min (◆), and 20°C/min (●).

gas at 60 mL/min was used during the experiments to purge the DSC cell. Samples between 15 and 20 mg were enclosed in aluminum DSC sample pans.

Dynamic scans were performed at four different heating rates 5, 10, 15, and 20°C/min from 15 to 300°C. The samples were then cooled to 15°C at a rate of 10°C/min. To complete the heat–cool–heat cycle, the samples were reheated to 300°C to confirm the nonexistence of any residual curing. Isothermal scans were performed at four different temperatures 110, 115, 117.5, and 120°C, determined from the dynamic DSC data. The isothermal scans were deemed to be complete when the thermograms leveled off to a baseline.

Sample preparation

EHO/TETA and EHO/TETA/IPD bioresin samples were prepared. For EHO/TETA samples, an equivalent ratio of epoxy groups to active amine hydrogen (EEW:AHEW) of 1 : 1 was used. Similarly for EHO/TETA/IPD samples, equivalent ratios of (EEW:AHEW:AHEW) of 1 : 0.5 : 0.5, was used. All of the constituents for each bioresin type were thoroughly mixed at room temperature. This process was repeated to prepare "fresh" samples for each DSC scan. EHO was completely miscible with both hardener systems.

Curing kinetics analysis theory

Dynamic curing kinetic models based on multiple heating rates, developed by Kissinger[18] and Ozawa–Flynn–Wall[23,24] along with an autocatalytic kinetic model developed by Kamal[25] were used in the kinetic analysis. DSC based cure kinetic analysis is dependent on the assumption that the heat flow, dH/dt is proportional to the reaction rate, $d\alpha/dt$. The degree of cure, α is proportional to the heat generated during the curing reaction. Therefore based on this assumption the curing reaction rate can be expressed as in eq. (1). Where, $d\alpha/dt$ is the reaction rate, t is time, $k(T)$ is the reaction rate constant that is an Arrhenius function of temperature and $f(\alpha)$ is the function that is dependent on α.

$$\frac{d\alpha}{dt} = k(T)f(\alpha) \tag{1}$$

The temperature dependence of $k(T)$ may be described by the Arrhenius expression, eq. (2). Where, A is the pre-exponential factor, E_a is the activation energy, R is the universal gas constant, and T is the absolute temperature in Kelvin.

$$k(T) = Ae^{-\frac{E_a}{RT}} \tag{2}$$

RESULTS AND DISCUSSION

Dynamic kinetic analysis: Kissinger and Ozawa–Wall methods

Both the Kissinger and Ozawa–Flynn–Wall methods were used in the dynamic kinetic analysis. Total reaction heat ΔH_{total} was determined as the area under the dynamic thermograms up to full conversion, Figures 3 and 4. The average total reaction heat was taken as the average of ΔH_{total} at each heating rate. The results in conjunction with the peak temperatures, T_m of the thermograms are summarized in Table I. T_m was determined from the peak of the exotherms at each heating rate using Universal Analysis 2000 version 3.9A software supplied with the DSC Q100.

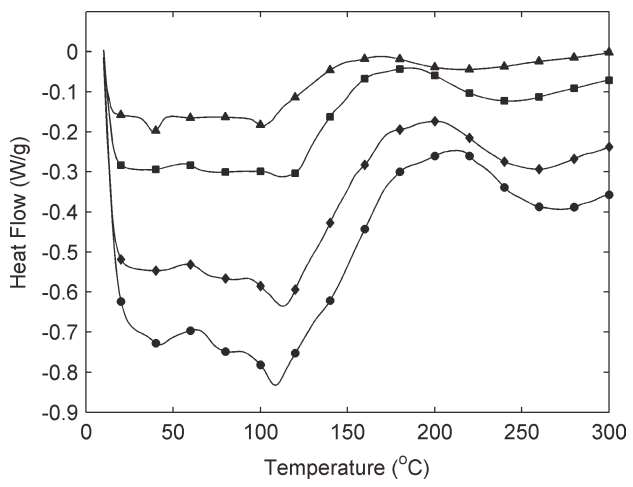

Figure 4 Dynamic DSC thermograms for EHO/TETA/IPD with 5°C/min (▲), 10°C/min (■), 15°C/min (◆), and 20°C/min (●).

TABLE I
Total Reaction Heats and Peak Temperatures for Both EHO-Based Bioresins Systems at Different Heating Rates

	ΔH_{total} (J/g)		T_m (°C)	
q (°C/min)	TETA	TETA/IPD	TETA	TETA/IPD
5	87.4	93.2	157.2	144.9
10	94.6	94.3	168.4	159.9
15	106.6	96.2	182.9	173.8
20	120.8	104.0	195.3	185.7
Avg. ΔH_{total}	102.4	96.9		

IPD was found to influence ΔH_{total}, average ΔH_{total}, and T_m. ΔH_{total} was lower for EHO/TETA/IPD samples compared with EHO/TETA with the exception of 5°C/min with EHO/TETA samples displaying a higher variation of ΔH_{total} over the heating rate range than EHO/TETA/IPD samples. Slightly lower values of average ΔH_{total} were observed for samples containing TETA/IPD compared with TETA samples indicating an influence by IPD. Overall, the TETA system displayed a wider dispersion of ΔH_{total} than the IPD system. Values of T_m showed a similar range for both sample types with TETA/IPD samples displaying lower values throughout the range. Similar findings in terms of the influence of IPD on ΔH_{total} and T_m were also reported by Czub.[26,27]

Based on Kissinger's proposal that α at the peak temperature is constant and independent of the heating rate, q for the curing reaction, the activation energy, E_a can be calculated from eq. (3). Whereby a plot of $\ln(q/T_m^2)$ versus $1/T_m$ will provide E_a without a specific assumption on the conversion-dependent function.[15]

$$\frac{d\left[\ln\left(q/T_m^2\right)\right]}{d(1/T_m)} = -\frac{E_a}{R} \tag{3}$$

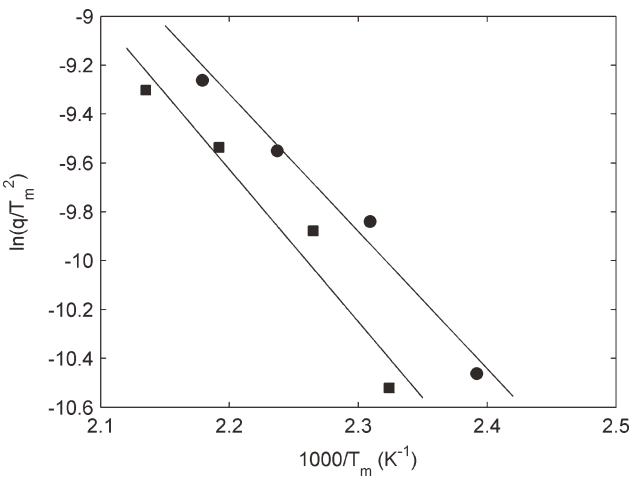

Figure 5 Activation energies obtained from Kissinger's method for EHO/TETA (■) and EHO/TETA/IPD (●).

An alternative kinetic model based on Doyle's approximation[28] was developed by Ozawa–Flynn–Wall, eq. (4). Where $g(\alpha)$ is a function dependent on α. A plot of log$q$ versus $1/T_m$ will provide E_a over the course of the reaction. To carry out the iso-conversional analysis using eq. (4), the reaction mechanism is assumed to be constant and $f(\alpha)$ in eq. (1) does not change at each point of conversion.

$$\log q = \log\left(\frac{AE_a}{g(\alpha)}\right) - 2.315 - \frac{0.4567E_a}{RT_m} \tag{4}$$

For both bioresin systems, peak temperatures and total heat of reactions were found to increase with increased heating rates as shown in Table I. Through application of Kissinger and Ozawa–Flynn–Wall methods, the activation energies were determined from the gradients of Figures 5 and 6 for both bioresin systems. Because of the observed linearity of the plots, validity of both models is suggested. Activation energies for both Kissinger and Ozawa–Flynn–Wall models proved to be similar for both systems.

Using the Kissinger model, values of 51.8 kJ/mol and 46.6 kJ/mol were obtained for EHO/TETA and EHO/TETA/IPD systems, respectively. From the Ozawa–Flynn–Wall model values of 56.3 kJ/mol and 51.3 kJ/mol were obtained for EHO/TETA and EHO/TETA/IPD systems respectively. These results are consistent with the findings of other researchers,[7,15,29,30] who also found activation energies from the Ozawa–Flynn–Wall model to be marginally higher than the values determined by the Kissinger model. These results show that the system containing IPD displays activation energies ~ 10% lower than the TETA/IPD system. This suggests that the addition of IPD enhances the curing reaction of the EHO bioresin system.

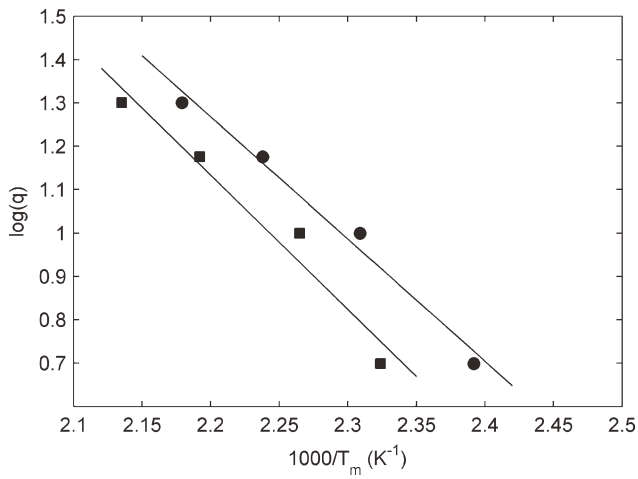

Figure 6 Activation energies obtained from Ozawa–Flynn–Wall method for EHO/TETA (■) and EHO/TETA/IPD (●).

TABLE II
Activation Energies (kJ/mol) and Pre-exponential Factors for Both Bioresin Systems

Bioresin system	E_{a1}	E_{a2}	A_1	A_2
EHO/TETA	139.5	−80.5	$e^{34.64}$	$e^{-31.69}$
EHO/TETA/IPD	114.7	−39.2	$e^{27.62}$	$e^{-20.15}$

Isothermal kinetic analysis: Autocatalytic model

Autocatalytic cure reaction models are used to model reactions where one of the reaction products is also a catalyst for further reactions.[31] Kamal's model[25] was found to accurately model both bioresin systems. This model has been successfully applied to numerous amine-cured systems and is shown in eq. (5). Where α is the degree of cure, k_1 and k_2 are the reaction rate constants, m and n are the reaction orders.[25] The nth order uncatalyzed and autocatalytic phenomena are accounted for by k_1 and k_2m, respectively.[32]

$$\frac{d\alpha}{dt} = (k_1 + k_2\alpha^m)(1-\alpha)^n \tag{5}$$

Postvitrification, some resin systems may be controlled by diffusion mechanisms rather than kinetic factors. Equation 5 can be modified to account for diffusion controlled mechanisms, eqs. (6) and (7).[33,34] Where C is a fitted constant and α_c is the critical conversion.

$$\frac{d\alpha}{dt} = (k_1 + k_2\alpha^m)(1-\alpha)^n g(\alpha) \tag{6}$$

$$g(\alpha) = \frac{1}{1 + e^{C(\alpha-\alpha_c)}} \tag{7}$$

Kamal's autocatalytic model modified to account for diffusion eq. (6), was used in this study. The kinetic parameter, k_1 was determined by extrapolating the isothermal reaction rate curves to $\alpha = 0$. The graphical-analytical, iterative method developed by Kenny[16] was used to determine the other associated kinetic parameters (k_2, m, and n).

Activation energies and pre-exponential factors were determined from the Arrhenius equation as described in our previous publication.[22] The data exhibited a linear form thereby indicating behavior predicted by eq. (2). Table II summarizes the activation energies and pre-exponential factors for both bioresin systems.

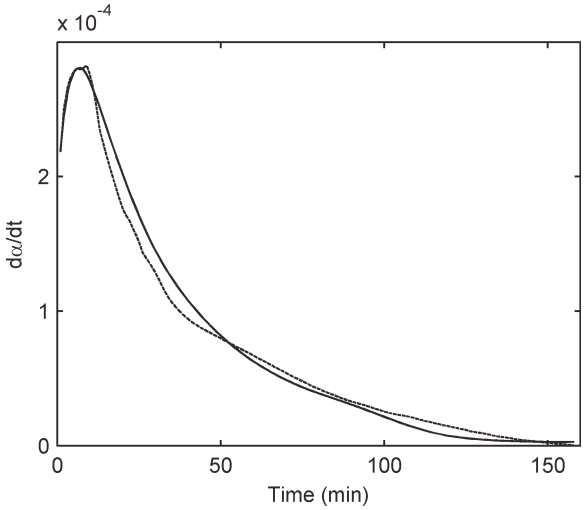

Figure 7 Comparison of experimental data (dashed line) with model predictions (solid line) for reaction rate versus time at 115°C for EHO/TETA.

The bioresin system containing IPD exhibits lower activation energy for E_{a1} than the system without IPD. Values of E_{a2} for both systems display anti-Arrhenius behavior as k_2 was found to decrease with temperature therefore implying a negative activation energy. This phenomenon was also previously observed and reported in our preceding publication and in our experiences is a phenomenon associated with curing of 100% EHO bioresin and not synthetic resins or blends.[22] The nature and cause of this behavior has not been identified although it is thought to be due to an unidentified competitive reaction that gives rise to the appearance of k_2 decreasing with increasing temperature.[35] Further investigation is required.

From Table III, it can be seen that as the temperature increased the values of k_1 increased and k_2 decreased for both systems. The higher magnitude of values for k_1 compared with k_2 for the TETA/IPD

TABLE III
Autocatalytic Model Parameters for Both Bioresin Systems

Sample	T (°C)	k_1	k_2	m	n	$m+n$	C	α_c
EHO/TETA	110.0	0.00010	0.00166	0.80	4.37	5.17	100	0.59
	115.0	0.00020	0.00116	0.75	3.51	4.26	140	0.68
	117.5	0.00025	0.00101	0.74	2.30	3.04	170	0.79
	120.0	0.00030	0.00087	0.71	1.64	2.35	200	0.90
EHO/TETA/IPD	110.0	0.00021	0.00053	1.02	2.87	3.89	80	0.65
	115.0	0.00031	0.00046	0.92	2.65	3.57	105	0.75
	117.5	0.00040	0.00043	0.86	1.70	2.56	120	0.88
	120.0	0.00053	0.00038	0.71	1.38	2.09	130	0.94

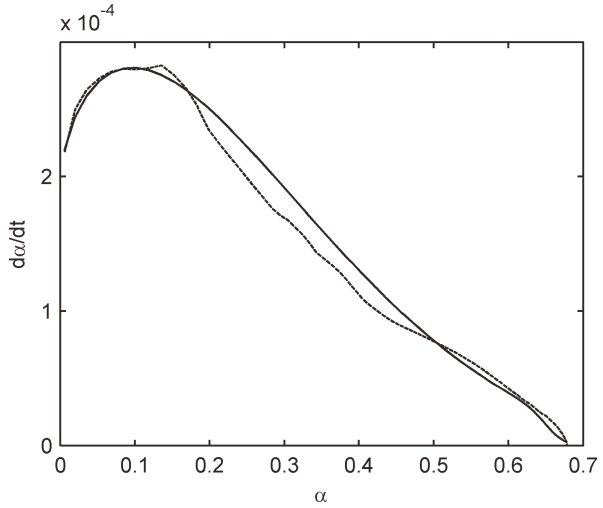

Figure 8 Comparison of experimental data (dashed line) with model predictions (solid line) for reaction rate versus degree of cure at 115°C for EHO/TETA.

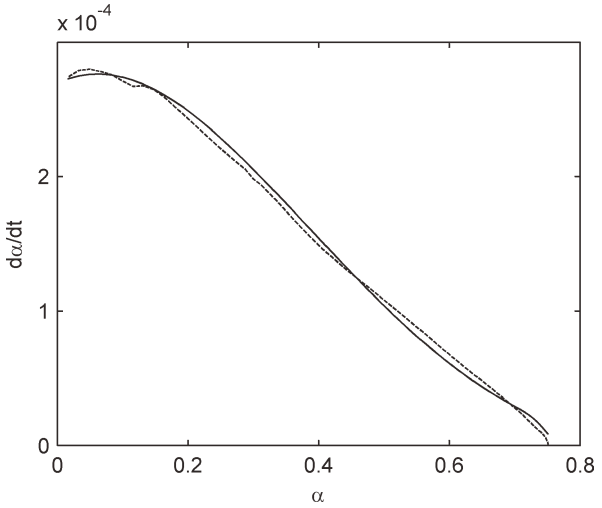

Figure 10 Comparison of experimental data (dashed line) with model predictions (solid line) for reaction rate versus time at 115°C for EHO/TETA/IPD.

system indicates that the reaction mechanism is more *n*th order dominant than autocataltyic. This can also be observed from Figures 7–10 whereby it is evident that the maximum reaction rate occurs closer to the beginning rather than in the intermediate conversion stage. Figures 7–10 display plots of experimental data and model predictions for both bioresin systems at 115°C. Similar results were obtained throughout this study at all temperatures. Good agreement of fit between experimental data with the autocatalytic model is observed throughout the entire temperature range for both systems. Values of m and n were found to decrease when the temperature increased for both systems. Subsequently, the overall reaction order was found to decrease with an increase in temperature. Average total reaction orders ($m + n$) were found to be $\sim$ 3.7 and 3.0 for the EHO/TETA and EHO/TETA/IPD, respectively. Throughout the entire temperature range, TETA/IPD based samples displayed higher conversions than TETA samples which can be seen in Figures 11 and 12.

CONCLUSIONS

An EHO-based bioresin system cured with two different systems; TETA and TETA/IPD was studied and compared. Cure kinetic analysis was performed using two dynamic models; Kissinger and Ozawa–Flynn–Wall and one autocatalytic model developed by Kamal modified to account for diffusion postvitrification. It was found that the total heats of reaction were slightly influenced by the addition of IPD. From the observed dynamic activation energies, the

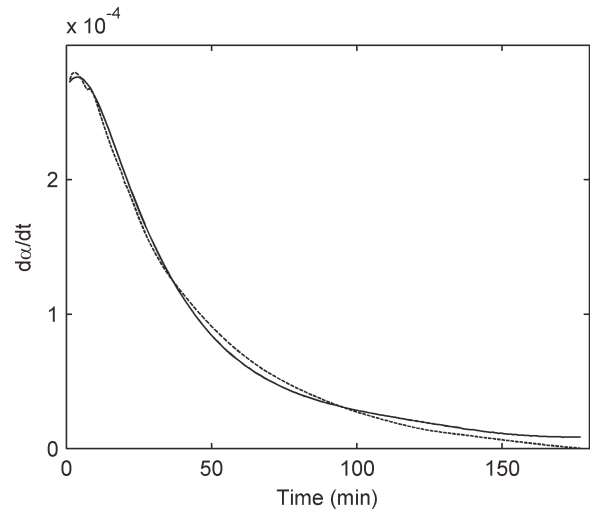

Figure 9 Comparison of experimental data (dashed line) with model predictions (solid line) for reaction rate versus time at 115°C for EHO/TETA/IPD.

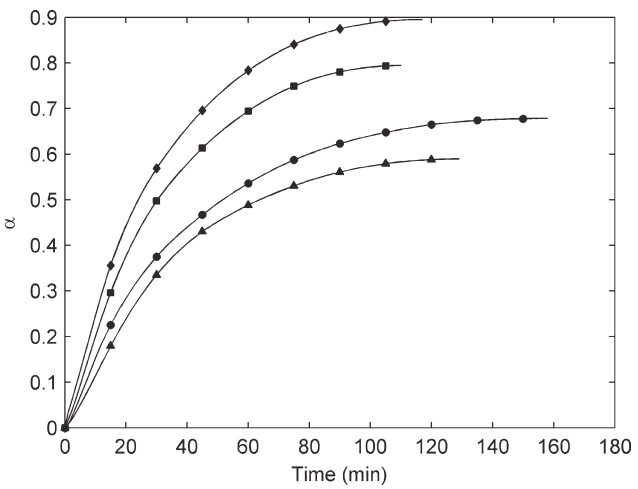

Figure 11 Degree of cure (α) as a function of time for EHO/TETA at 110°C (▲), 115°C (●), 117.5°C (■), and 120°C (◆).

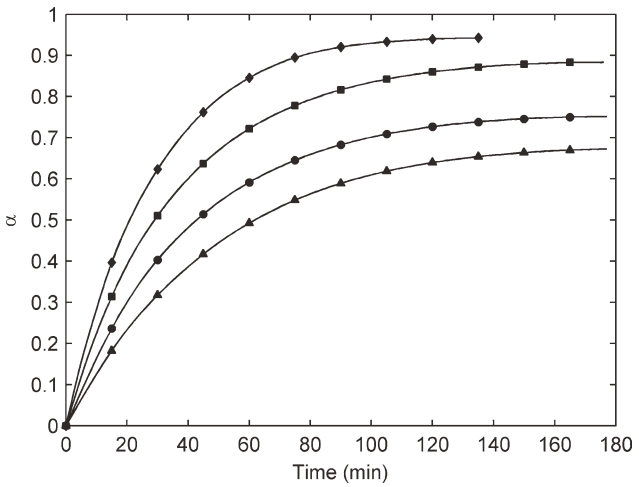

Figure 12 Degree of cure (α) as a function of time for EHO/TETA/IPD at 110°C (▲), 115°C (●), 117.5°C (■), and 120°C (◆).

bioresin system containing IPD exhibited activation energies ~ 10% lower than the TETA system.

Both bioresin systems displayed autocatalytic mechanisms with the system containing IPD being characterized as heavily influenced by *n*th order mechanicsms. Maximum conversions of the TETA/IPD system were consistantly higher than those of the TETA system throughout the entire temperature range. Cure kinetic parameters where obtained for both systems with k_1 and k_2 increasing and decreasing, respectively, as temperature increased. The observed decrease in k_2 is thought to be due to an unidentified competive reaction. The total order of the reaction was found to decrease with an increase in temperature for both systems. An autocatalytic model developed by Kamal, modified to account for diffusion postvitrification was found to satisfactorily describe the cure behavior of both systems. It was found that IPD increased the curing rate of the EHO bioresin systems.

The first author would like to thank the Queensland State Government for providing a Smart Futures PhD Scholarship to make this research possible.

References

1. Miyagawa, H.; Misra, M.; Drzal, L. T.; Mohanty, A. K. Polym Eng Sci 2005, 45, 487.
2. Miyagawa, H.; Mohanty, A. K.; Misra, M.; Drzal, L. T. Macromol Mater Eng 2004, 289, 636.
3. Chandrashekhara, K.; Sundararaman, S.; Flanigan V.; Kapila, S. Mater Sci Eng A 2005, 412, 2.
4. Zhu, J. K.; Chandrashekhara, K.; Flanigan, V.; Kapila, S. Compos A 2004, 35, 95.
5. Espinoza-Pérez, J.; Wiesenborn, D.; Ulven, C.; Haagenson, D.; Brudvik, R. 2009 ASABE Annual International Meeting, Reno, Nevada, June 21–24, 2009.
6. Morye, S. S.; Wool, R. P. Polym Compos 2005, 26, 407.
7. Chen, W. Y.; Wang, Y. Z.; Chang, F. C. J Appl Polym Sci 2003, 92, 892.
8. Ramos, J. A.; Pagani, N.; Riccardi, C. C.; Borrajo, J.; Goyanes, S. N.; Mondragon, I. Polymer 2005, 46, 3323.
9. Rosu, D.; Mititelu, A.; Cascaval, C. N. Polym Test 2004, 23, 209.
10. Ghaemy, M.; Barghamadi, M.; Behmadi, H. J Appl Polym Sci 2004, 94, 1049.
11. Du, S.; Guo, Z. S.; Zhang, B.; Wu, Z. Polym Int 2003, 53, 1343.
12. Ghaemy, M.; Rostami, A. A.; Omrani, A. 2005, 55, 279.
13. Vyazovkin, S.; Sbirrazzuoli, N. Macromol Chem Phys 1999, 200, 2294.
14. Vyazovkin, S.; Sbirrazzuoli, N. Macromolecules 1996, 29, 1867.
15. Barral, L.; Cano, J.; López, J.; López-Bueno, I.; Nogueira, P.; Abad, M. J.; Ramírez, C. J Polym Sci Part B: Polym Phys 2000, 38, 351.
16. Kenny, J. M. J Appl Polym Sci 1994, 51, 761.
17. Kenny, J. M.; Trivisano, A. Polym Eng Sci 1991, 31, 1426.
18. Kissinger, H. E. Anal Chem 1957, 29, 1702.
19. Liang, G.; Chandrashekhara, K. J Appl Polym Sci 2006, 102, 3168.
20. Liang, G.; Garg, A.; Chandrashekhara, K.; Flanigan, V.; Kaplia, S. J Reinf Plast Compos 2005, 24, 1509.
21. Park, S. J.; Jin, F. L.; Lee, J. R. Macromol Rapid Commun 2004, 25, 724.
22. Manthey, N. W.; Cardona, F.; Aravinthan, T.; Cooney, T. J Appl Polym Sci 2011, 121:n/a, doi 10.1002/app.34086.
23. Ozawa, T. J Therm Anal Calorim 1970, 2, 301.
24. Flynn, J. H.; Wall, L. A. J Res Natl Bur Stand Sect A 1966, 42, 487.
25. Kamal, M. R. Polym Eng Sci 1974, 14, 231.
26. Czub, P. Macromol Symp 2006, 242, 60.
27. Czub, P. Macromol Symp 2006, 245, 533.
28. Doyle, C. D. Nature 1965, 3, 290.
29. Martini, D. S.; Braga, B. A.; Samios, D. Polymer 2009, 50, 2919.
30. Islam, M. S.; Pickering, K. L.; Foreman, N. J. J Adhes Sci Technol 2009, 23, 2085.
31. Pan, H.; Shupe, T. F.; Hse, C. Y. J Appl Polym Sci 2008, 108, 1837.
32. Karayannidou, G. E.; Achilias, D. S.; Sideridou, I. D. Eur Polym J 2006, 42, 3311.
33. Chern, C. S.; Poehlein, G. W. Polym Eng Sci 2004, 7, 788.
34. Cole, K. C. Macromolecules 1991, 24, 3093.
35. Helfferich, F. G. Kinetics of Multistep Reactions, 2nd ed.; Elsevier: Amsterdam, 2004; Chap. 13, pp 429–432.